

# Finite element analysis of convective Heat and Mass transfer flow of Rotating fluid past a vertical Stretching plate with Second Order Slip

**Dr. Y. Devasena**

*Assistant Professor, School of Engineering & Technology  
Sri Padmavathi Mahila Visvavidyalayam, Tirupathi-517502, A.P., India*

**Dr. A. Haritha**

*Assistant Professor, School of Engineering & Technology  
Sri Padmavathi Mahila Visvavidyalayam, Tirupathi-517502, A.P., India*

**Abstract:** In this paper we analysed the effect of second order slip on hydromagnetic convective heat and mass transfer flow of viscous electrically conducting rotating fluid in a vertical rotating plate in the presence of transverse magnetic field with Soret and Dufour effects. By employing finite element technique the equations governing the flow, heat and mass transfer have been solved. The velocity, temperature, concentration are analysed for different parametric values. The shear stress, rate of heat and mass transfer on the boundary are evaluated numerically for different variations.

**Keywords :** Second order slip, Rotating fluid, Soret and Dufour effects, Dissipation, Constant Heat and Mass flux.

## 1. INTRODUCTION:

The motion of rotation fluids enclosed with in a body or vice versa, was given by Green span, discussed these problems relating to the boundary layers and their interaction in rotating flows and gave so many examples relating to such interaction. Rao et.al. [20] made an investigation of the combined free and forced convective effects on an unsteady Hydro magnetic viscous incompressible flow in a rotating porous channel. This analysis has been extended to porous boundaries by Sarojamma and Krishna[22]. An initial value investigation of the hydro magnetic and convective flow of a viscous electrically conducting fluid through a porous medium in a rotating channel has been made by Krishna et.al. [10]. In all these papers the viscous dissipative effect has not been considered. But the viscous dissipation has its importance when the natural convection flow fixed is of extreme size or the temperature is low or in higher gravity field. Seth and Ghosh [24] has investigated the unsteady hydromagnetic flow of viscous incompressible electrically conducting fluid in rotating channel under the influence of periodic pressure gradient and of uniform magnetic field, which is inclined with the axes of rotation. Hazim Ali Attia [9] has developed the MHD flow of incompressible, viscous and electrically conducting fluid above an infinite rotating porous disk was extended to flow starting impulsively from rest. Circar and Mukherjee [5] have analyzed the effect of mass transfer and rotation on flow past a porous plate in a porous medium with variable suction in a slip flow regime. Balasubramanyam [3] and Madhusudhan Reddy [14] have investigated convective heat and mass transfer flow in horizontal rotating fluid under different conditions. Singh and Mathew [25] have studied on oscillatory free convective MHD flow in a rotating vertical porous channel with heat sources. The effect of Hall currents on convective flows in rotating fluid have been attempted by several authors [1,2,6,10,13,19,24,27,26].

In all the abovementioned investigations, the no-slip conditions are employed. However it is noticed in a micro electro mechanical systems and some coated surfaces(such as Teflon, resist adhesion)the no-slip boundary condition is adequate .Especially partial slip condition is important in the situation when the fluid is particulate such as emulsions, suspensions, foams and polymer solution. Undoubtedly the materials exhibiting slip are important in technological applications such as in the polishing of artificial heart valves and internal cavities. A similar of models have proposed for describing the slip effect that occurs at solid boundaries. The slip flow model describes a relation between the tangential component of the velocity at the surface and velocity gradient normal to the surface. Thus a new dimension is added to the above mentioned study by considering the effects of partial slip at the stretching wall. Turkyilmazoglu [28] found the multiple solutions for the heat and mass transfer effects in MHD flow of viscoelastic fluid over a stretching wall with slip boundary condition. Freidoonimehr et al [7] analysed the HD stagnation point flow towards a porous rotating sheet with velocity slip condition. Turkyilmazoglu [29] investigated the heat and mass transfer characteristics in MHD viscous flow

over a permeable stretche3d surface with velocity and thermal slip conditions. Mukhopadhyay [16] performed an analysis to study the slip effects in MHD boundary layer flow over a porous stretching sheet with thermal radiation. Malvandi [15] examined the stagnation point flow of nano-fluid over a stretched surface with Navier's slip condition. Mabood et al [11] considered melting heat transfer on MHD flow of nano-fluid with radiation and second order slip. The slip effect in mixed convective boundary layer flow over a flat surface is studied by Bhattacharya et al [4]. Rashid et al [21] studied the effects of magnetohydrodynamic in flow by a rotating dish with slip effect. Mukhopadhyay [17] examined the MHD axi-symmetric flow of a viscous fluid by a stretched cylinder with heat transfer and partial slip effect. Flow of second -grade fluid past a stretching sheet with partial slip is addressed by Hayat et al [8]. Mabood et al [12] have discussed the radiation effect on stagnation point flow with melting heat transfer with second order slip.

**2. FORMULATION OF THE PROBLEM**

We consider a steady hydromagnetic heat and mass transfer flow of a viscous electrically conducting along a porous infinite vertical plate  $y=0$  in a rotating system. The flow is also assumed to be moving with a uniform velocity  $U_\infty$ , which is in the  $x$ -direction, is taken along the plate in the upward direction and the  $y$ -axis is normal to it. Initially the plate is at rest, after that the whole system is allowed to rotate with a constant angular velocity  $\Omega$  about the  $y$ -axis. The temperature and the species concentration at the plate are constantly raised from  $T_\infty$  and  $C_\infty$  to  $T_w$  and  $C_w$  respectively, where  $T_\infty$  and  $C_\infty$  are the temperature and species concentration of the uniform flow respectively. A uniform magnetic field  $B$  is taken to be along the  $y$ -axis which is assumed to be electrically non-conducting. We assumed following (Pai [18]) that the magnetic Reynolds number of the flow is taken to be small enough so that the induced magnetic field is negligible in comparison with applied one, so that  $B=(0,B_0,0)$  and the magnetic lines of force are fixed relative to the fluid. The equation of conservation of charge  $\nabla \cdot \vec{J} = 0$  gives  $J_y = \text{constant}$ , where the current density  $\vec{J} = (J_x, J_y, J_z)$ . Since the plate is electrically non-conducting, this constant is zero and hence  $J_y = 0$  at the plate and also zero everywhere. A uniform magnetic field in the

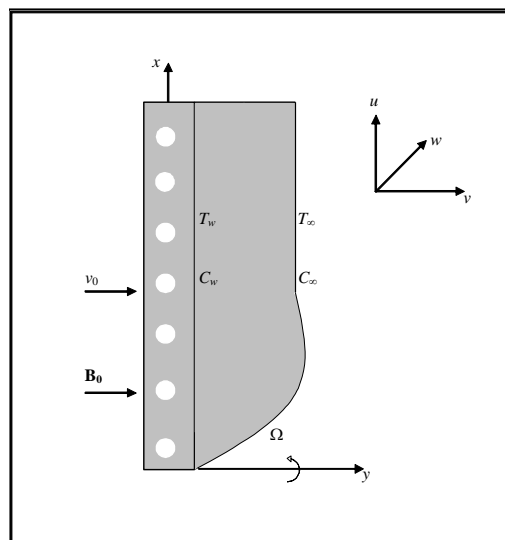


Fig. 1 : Physical configuration and coordinate system

The physical configuration considered here is shown in Fig. 1. It is assumed that the plate is semi-infinite in extent and hence all the physical quantities depend on  $y$  and  $x$ . Taking Hall currents into account the governing equations under Boussinesq's approximation are

$$\frac{\partial u}{\partial x} + \frac{\partial v}{\partial y} = 0 \tag{2.1}$$

$$u \frac{\partial u}{\partial x} + v \frac{\partial u}{\partial y} + 2\Omega w = v \left( \frac{\partial^2 u}{\partial y^2} \right) + \frac{\sigma B_0^2}{1+m^2} ((u - U_o) - mw) + \beta g(T - T_\infty) + \beta^* g(C - C_\infty) - \left( \frac{v}{k} \right) u \tag{2.2}$$

$$u \frac{\partial w}{\partial x} + v \frac{\partial w}{\partial y} + 2\Omega(U_o - u) = v \left( \frac{\partial^2 w}{\partial y^2} \right) - \frac{\sigma B_0^2}{1+m^2} (mw - (u - U_o) - \left( \frac{v}{k} \right) w) \tag{2.3}$$

$$u \frac{\partial T}{\partial x} + v \frac{\partial T}{\partial y} = \frac{k_f}{\rho C_p} \frac{\partial^2 T}{\partial y^2} + \frac{v}{C_p} \left( \left( \frac{\partial u}{\partial y} \right)^2 + \left( \frac{\partial w}{\partial y} \right)^2 \right) - Q_H(T - T_\infty) + \frac{\sigma B_0^2}{C_p(1+m^2)} (u^2 + w^2) + \frac{D_m K_T}{C_s C_p} \frac{\partial^2 C}{\partial y^2} \tag{2.4}$$

$$u \frac{\partial C}{\partial x} + v \frac{\partial C}{\partial y} = D_m \frac{\partial^2 C}{\partial y^2} + \frac{D_m K_T}{T_m} \frac{\partial^2 T}{\partial y^2} \tag{2.5}$$

The boundary conditions for the problem are

$$u = bx + A' \frac{\partial u}{\partial y} + B' \frac{\partial^2 u}{\partial y^2}, v = -v_w, w = 0, \frac{\partial T}{\partial y} = -\frac{q_w}{k_f}, \frac{\partial C}{\partial y} = -\frac{q_m}{D_B} \quad \text{at } y=0$$

$$u = U_0, \quad w=0, \quad T \rightarrow T_\infty, C \rightarrow C_\infty \text{ as } y \rightarrow \infty \quad (2.6)$$

where  $b > 0$ . The boundary conditions on the velocity in (2.6) are the no-slip conditions at the surface at  $y=0$ , while the boundary conditions on the velocity as  $y \rightarrow \infty$  follow from the fact that there is no flow far away from the stretching surface. The temperature and species concentration are maintained at a prescribed constant values  $T_w$  and  $C_w$  at the sheet and are assumed to vanish far away from the sheet.

Following the work of Sattar [23], a transformation is now made as

$$u_1 = U_0 - u \quad \Rightarrow \quad u = U_0 - u_1 \quad (2.7)$$

Equations (2.1)-(2.5) and the boundary conditions (2.6), respectively, transform to

$$-\frac{\partial u_1}{\partial x} + \frac{\partial v}{\partial y} = 0 \quad (2.8)$$

$$(U_0 - u_1) \frac{\partial u}{\partial x} + v \frac{\partial u}{\partial y} + 2\Omega w = \nu \left( \frac{\partial^2 u_1}{\partial y^2} \right) + \frac{\sigma B_0^2}{1+m^2} (u_1 - mw) + \quad (2.9)$$

$$+ \beta g (T - T_\infty) + \beta^* g (C - C_\infty) - \left( \frac{\nu}{k} \right) (U_0 - u_1)$$

$$(U_0 - u_1) \frac{\partial w}{\partial x} + v \frac{\partial w}{\partial y} + 2\Omega u_1 = \nu \left( \frac{\partial^2 w}{\partial y^2} \right) - \frac{\sigma B_0^2}{1+m^2} (mw - u_1) - \left( \frac{\nu}{k} \right) w \quad (2.10)$$

$$(U_0 - u_1) \frac{\partial T}{\partial x} + v \frac{\partial T}{\partial y} = \frac{k_f}{\rho C_p} \frac{\partial^2 T}{\partial y^2} - Q_H (T - T_\infty) + \frac{\nu}{C_p} \left( \left( \frac{\partial u_1}{\partial y} \right)^2 + \left( \frac{\partial w}{\partial y} \right)^2 \right) + \quad (2.11)$$

$$+ \left( \frac{\sigma B_0^2}{C_p (1+m^2)} \right) (u_1^2 + w^2) + \frac{D_m K_T}{C_s C_p} \frac{\partial^2 C}{\partial y^2}$$

$$(U_0 - u_1) \frac{\partial C}{\partial x} + v \frac{\partial C}{\partial y} = D_m \frac{\partial^2 C}{\partial y^2} + \frac{D_m k_T}{T_m} \frac{\partial^2 T}{\partial y^2} \quad (2.12)$$

$$u_1 = ax + A' \frac{\partial u}{\partial y} + B' \frac{\partial^2 u}{\partial y^2}, v = v_0(x), w = 0, \frac{\partial T}{\partial y} = -\frac{q_w}{k_f}, \frac{\partial c}{\partial y} = -\frac{q_m}{D_B} \quad \text{at } y=0$$

$$u_1 = 0, \quad w=0, \quad T \rightarrow T_\infty, C \rightarrow C_\infty \text{ as } y \rightarrow \infty \quad (2.13)$$

where  $u, v, w$  are the velocity components in the  $x, y, z$  directions respectively,  $\nu$  is the kinematic viscosity,  $g$  is the acceleration due to gravity,  $\rho$  is the density,  $\beta$  is the coefficient of volumetric thermal expansion,  $\beta^*$  is the volumetric mass expansion.  $T, T_w, T_\infty$  are the temperature of the fluid inside the thermal boundary layer, the plate temperature and the fluid temperature in the free stream respectively, while  $C, C_w, C_\infty$  are the corresponding concentrations. Also,  $k$  is the permeability of the porous medium.  $k_f$  is the thermal conductivity of the medium,  $D_m$  is the coefficient of mass diffusivity,  $T_m$  is the thermal diffusion ratio,  $C_p$  is the specific heat at constant pressure,  $T_m$  is the mean fluid temperature,  $k_T$  is the thermal diffusion ratio,  $C_p$  is the concentration,  $C_s$  is the concentration susceptibility and  $Q_H$  is the strength of the temperature dependent heat source.

### 3. MATHEMATICAL ANALYSIS

In order to solve equations (2.9)-(2.12) under the boundary conditions (2.13), we adopt the well-defined similarity analysis to attain similarity solutions.

For this purpose, the following similarity transformations are now introduced:

$$\eta = y \sqrt{\frac{U_o}{2\nu x}}, \quad g_o(\eta) = \frac{w}{U_o}, \quad \theta(\eta) = \frac{T - T_\infty}{(k_f / q_w)}, \quad \phi(\eta) = \frac{C - C_\infty}{(D_B / m_w)},$$

$$\psi = \sqrt{2\nu x U_o} f(\eta), \quad u_1 = \frac{\partial \psi}{\partial y} = U_o f'(\eta), \quad \frac{u}{U_o} = 1 - f'(\eta) \quad (2.14)$$

Now for reasons of similarity, the plate of concentration is assumed to be

$$C_w(x) = C_o + \bar{x}(C_o - C_\infty)$$

where  $C_o$  is considered to be mean concentration and  $\bar{x} = \frac{xU_o}{\nu}$

The continuity equation (2.1) then yields

$$v = \frac{\partial \psi}{\partial x} = -\sqrt{\frac{\nu U_o}{2x}} (\eta f'(\eta) - f(\eta)) \quad (2.15)$$

$$\text{Also we have } f_w = v_w(x) \sqrt{\frac{2x}{\nu U_o}} \quad (2.16)$$

Where  $f_w$  is the suction parameter or transpiration parameter and clearly in (2.16)  $f_w < 0$  corresponds to suction and  $f_w > 0$  corresponds to injection at the plate. Using (2.14) in equations (2.9)-(2.12), we have the following dimensionless ordinary coupled non-linear differential equations.

$$f''' + (\eta - f')f'' - Gr(\theta + N\phi) + Rg_o - Kf' - \frac{M^2}{1+m^2}(f' + mg) = 0 \quad (2.17)$$

$$g_o'' + (\eta - f)g_o' + Rf' - Kg_o - \frac{M^2}{1+m^2}(mg_o - f') = 0 \quad (2.18)$$

$$\theta'' + P_r(\eta - f)\theta' - Q\theta + P_r Ec((f'')^2 + (g_o')^2) + \frac{Pr Ec M^2}{1+m^2}((f')^2 + (g_o)^2) + Du\phi'' = 0 \quad (2.19)$$

$$\phi'' + Sc(\eta - f)\phi' + 2Sc(f'\phi) + ScS_r\theta'' = 0 \quad (2.20)$$

With the corresponding boundary conditions

$$f = f_w f'(0) = 1 + Af''(0) + Bf'''(0), \quad g_o = 0, \quad \frac{d\theta}{d\eta} = -1, \quad \frac{d\phi}{d\eta} = -1 \quad \text{at } \eta = 0$$

$$f' = 0, \quad g_o = 0, \quad \theta = 0, \quad \phi = 0 \quad \text{as } \eta \rightarrow \infty \quad (2.21)$$

where

$$Gr = \frac{2\beta g(T_w - T_\infty)x^3}{\nu^2}, \quad N = \frac{\beta(C_w - C_\infty)}{\beta(T_w - T_\infty)}, \quad M^2 = \frac{2x\sigma B_o^2}{\rho U_o}, \quad M_1^2 = \frac{M^2}{1+m^2}$$

$$R = \frac{4\Omega x}{U_o}, \quad K = \frac{kU_o}{2\nu x}, \quad Q = \frac{2Q_H x \nu}{k_f}, \quad Pr = \frac{\rho \nu C_p}{k_f}, \quad Ec = \frac{U_o^2}{C_p(T_w - T_\infty)}, \quad Sc = \frac{\nu}{D_m},$$

$$S_r = \frac{D_m K_T(T_w - T_\infty)}{T_m(C_w - C_\infty)}, \quad Du = \frac{D_m K_T(C_w - C_\infty)}{C_s C_p(T_w - T_\infty)}$$
 are Grashof number, Buoyancy parameter, Magnetic

parameter, Rotation parameter, Porous permeability parameter, Heat source parameter, Prandtl number, Eckert parameter, Schmidt number, Soret parameter, Dufour parameter respectively. For the computational purpose and without loss of generality  $\infty$  has been fixed as 8. The whole domain is divided into 11 line elements of equal width, each element being three noded.

#### 4. FINITE ELEMENT ANALYSIS

The finite element analysis with quadratic polynomial approximation functions is carried out along the axial direction. The behavior of the velocity, temperature and concentration profiles has been discussed computationally for different variations in governing parameters. The Galerkin method has been adopted in the

variational formulation in each element to obtain the global coupled matrices for the velocity, temperature and concentration in course of the finite element analysis.

Choose an arbitrary element  $e_k$  and let  $u^k, \theta^k$  and  $C^k$  be the values of  $u, \theta$  and  $C$  in the element  $e_k$ . We define the error residuals as

$$E_f^k = \frac{df}{d\eta} - h \tag{3.1}$$

$$E_h^k = \frac{d}{d\eta} \left( \frac{dh}{d\eta} \right) + (\eta - h) \frac{dh}{d\eta} - G(\theta + N\phi) - Rg_o - D^{-1}h - M_1^3(h + mg_o) \tag{3.2}$$

$$E_g^k = \frac{d}{d\eta} \left( \frac{dg}{d\eta} \right) + (\eta - h) \frac{dg}{d\eta} + Rh - M_1^2(g_o - mh) - D^{-1}g_o \tag{3.3}$$

$$E_\theta^k = \frac{d}{d\eta} \left( \frac{d\theta}{d\eta} \right) + (\eta - f) P_r \frac{d\theta}{d\eta} + Pr Ec ((h')^2 + (g_o)^2) - Q\theta + Du \frac{d}{d\eta} \left( \frac{d\phi}{d\eta} \right) + Pr Ec \left( \frac{M^2}{1+m^2} + D^{-1} \right) (h^2 + (g_o)^2) \tag{3.4}$$

$$E_\phi^k = \frac{d}{d\eta} \left( \frac{d\phi}{d\eta} \right) + Sc(\eta - f) \frac{d\phi}{dy} + 2Sc(h\phi + ScSr \frac{d}{d\eta} \left( \frac{d\phi}{d\eta} \right)) \tag{3.5}$$

where  $f_k, h_k, \theta_k, \phi_k$  are values of  $f, h, \theta$  &  $\phi$  in the arbitrary element  $e_k$ . These are expressed as linear combinations in terms of respective local nodal values.

$f = \sum_{k=1}^3 f_k \psi_k, h = \sum_{k=1}^3 h_k \psi_k, \theta = \sum_{k=1}^3 \theta_k \psi_k, \phi = \sum_{k=1}^3 \phi_k \psi_k$  where  $\psi_1^k, \psi_2^k, \dots$  etc are Lagrange's quadratic

polynomials. Galerkin's method is used to convert the partial differential Equations (2.17)–(2.20) into matrix form of equations which results into 3x3 local stiffness matrices. All these local matrices are assembled in a global matrix by substituting the global nodal values of order I and using inter element continuity and equilibrium conditions.

The shear stress ( $\tau$ ), Nusselt number (rate of heat transfer), Sherwood number (rate of mass transfer) are evaluated by using the following formulas

$$\tau = \left( \frac{dh}{dr} \right)_{\eta=0}, Nu = 1/\theta(0), Sh = 1/\phi(0)$$

### 5.COMPARISON

In the absence of Hall currents ( $m=0$ ), Heat sources ( $Q=0$ ), Dufour parameter ( $Du$ ) and first and second order slips regime ( $A=0, B=0$ ) the results are in good agreement with Sreerangavani et al [26].

Table.1 shows the comparison

Parameters			Sreerangavani et al [26]			Present results( $m=0, Q=0, A=0, B=0$ )		
R	So	Ec	$\tau_x(0)$	Nu(0)	Sh(0)	$\tau_x(0)$	Nu(0)	Sh(0)
0.5	0.5	0.01	3.49064	0.07426	1.2087	3.48995	0.07429	1.2084
1.0	0.5	0.01	3.48376	<b>0.07328</b>	1.2079	3.48369	<b>0.07329</b>	1.2081
1.5	0.5	0.01	3.47259	<b>0.07164</b>	1.2054	3.47260	<b>0.07167</b>	1.2059
0.5	1.0	0.01	3.48853	0.07523	1.2761	3.48852	0.07521	1.2764
0.5	1.5	0.01	3.48704	0.07596	1.3214	3.48706	0.07599	1.3217
0.5	0.5	0.03	3.43136	0.08732	1.4987	3.43141	0.08728	1.4989
0.5	0.5	0.055	3.57222	0.05684	0.8670	3.57229	0.05686	0.8671
0.5	0.5	0.07	3.69426	0.03131	0.4445	3.69429	0.03132	0.4442

## 6. DISCUSSION OF THE NUMERICAL RESULTS

The non-linear linear equations governing the flow have been analysed by employing Galerkin finite element technique with three noded line segments. The parameters  $G, M, Sc, Pr$  are taken as 2, 0.5, 1.3 and 0.71 respectively. The velocity, temperature and concentrations distributions have been analysed for different variations of the parameters  $m, \gamma, Q, Ec, R, A, B$  and  $Sr$  and  $Du$ .

Figs. 2-8 show the variation of the axial velocity ( $u/U_0$ ) with different values of,  $m, N, Q, \gamma, Ec, R, A, B, Sr$  and  $Du$ . An increase in the Hall parameter ( $m$ ) decreases the axial velocity in the flow region (fig. 2a). When the molecular buoyancy force dominates over the thermal buoyancy force primary secondary velocities, temperature and concentration enhances when the buoyancy forces are in the same directions and for the forces in opposite directions, primary velocity, temperature and concentration reduces, secondary velocity enhances in the 3 flow region (fig. 3a). Fig. 4a represent  $f^1(\eta)$  with rotation parameter  $R$ . It can be observed from the profiles that ( $u/U_0$ ) enhances with increase in the rotation parameter  $R$ . Fig. 5a shows the variation of axial velocity with heat source parameter ( $Q$ ). From the profiles we find that in the presence of heat generating source, the velocity reduces and enhances with absorbing source in the region (0,1). In the remaining region (1,4), it enhances with increase in the strength of the heat generating/absorbing source. With reference to  $Ec$ , it can be seen that higher the dissipative heat smaller the velocity. Thus the presence of the dissipative term leads to a depreciation in the axial velocity (fig. 6a). Increasing the Soret parameter  $S_r$  (or decreasing Dufour parameter  $Du$ ) smaller the axial velocity in the flow region (fig. 6a). From (fig. 8a) we find that an increase in slip parameter ( $A$ ) reduces the axial velocity in the flow region (0,1.5) and increases in the remaining region while the axial velocity enhances in the region (0,1.0) and reduces in the region (1,4) with increase in the secondary slip parameter ( $B$ ) (fig. 9a). Thus the effect of secondary slip parameter ( $B$ ) in flow region is opposite to the that of first order slip parameter ( $A$ ).

The cross velocity ( $g(\eta)$ ) which arises due to the rotation and Hall current is shown in figures for different parametric values. It is found that the cross velocity  $g(\eta)$  enhances with increase in  $m, N > 0$  (fig. 3b, 4b) and reduces with,  $R, Ec, N < 0$  (fig. 3b, 4b, 6b). From fig. 5b we find that the cross velocity enhances in the flow region (0,1.5) and reduces in the region (1.5, 4.0) with increase in the strength of heat generating/absorbing source. Increasing  $S_r$  (or decreasing  $Du$ ) leads to an enhancement in  $g(\eta)$  (fig. 7b). The cross velocity enhances with  $A$  and reduces with  $B$  in the region (0,1.5) and a reversed effect is noticed in the remaining region (figs. 8b, 9b). Thus the effect of secondary slip parameter ( $B$ ) on  $g(\eta)$  is opposite the behaviour of  $g(\eta)$  with first slip parameter ( $A$ ).

The non-dimensional temperature ( $\theta$ ) is shown in figures for different parametric values. Higher the Hall parameter ( $m$ ) smaller the temperature in the flow region (fig. 2c). The temperature reduces with  $N > 0$  and enhances with  $N < 0$  (fig. 4c). From fig. 5c we find that the temperature enhances in the case of heat generating source ( $Q > 0$ ) and reduces with  $Q < 0$ . Increasing the Soret parameter  $S_r$  (or decrease in  $Du$ ) results in a depreciation in the temperature (fig. 7c). Higher the first order slip parameter ( $A$ ) smaller while the secondary slip parameter ( $B$ ) increases the temperature in the flow region (8c & 9c). Thus the effect of secondary slip parameter on  $\theta$  is opposite to that of first order parameter. An increase in rotation parameter  $R$  / Eckert number  $Ec$  leads to an enhancement in the temperature (figs. 4c, 6c).

The concentration distribution ( $C$ ) is shown in figures 2d-8d for different parametric values. We follow the convention that the non-dimensional concentration is positive/negative according as actual concentration is greater/lesser than the ambient concentration. It is found that an increase in  $m$  leads to a depreciation in the actual concentration (figs. 2d). The concentration reduces with buoyancy ratio ( $N > 0$ ) and enhances with  $N < 0$  (fig. 3d). From figs. 4d we find that the actual concentration enhances with  $R$ . Increasing Soret parameter  $S_r (\leq 1.5)$  (or decrease in  $Du$ ) leads to a depreciation and for higher  $S_r (\geq 2.0)$  larger actual concentration in the flow region (0, 0.75) while in the remaining region (0.8, 4.0) it enhances with  $S_r$  (or  $Du$ ) (fig. 7d). From fig. 5d we find that the actual concentration enhances with  $Q > 0$  and reduces with  $Q < 0$  in the flow region (0, 1.5) and a reversed effect is noticed in the remaining region. From fig. 6d we find that the concentration reduces with Eckert number  $Ec$  and first order slip parameter ( $A$ ) (8d). An increase in the secondary slip parameter ( $B$ ) enhances the actual concentration (fig. 9d).

The components of skin friction  $\tau_x$  &  $\tau_z$ , Nusselt and Sherwood numbers at the wall  $\eta=0$  are depicted in tables 2 for different values of,  $m, R, Ec, Sr, Du, A, B$ . It is found that  $\tau_x, \tau_z, Nu$  and  $Sh$  enhances with increase in Hall parameter ( $m$ )/rotation parameter ( $R$ ). The variation of stress components with heat source parameter ( $Q$ ) shows that both the components,  $Nu$  and  $Sh$  enhance in the presence of heat generating source while  $\tau_x, \tau_z, Nu$  reduces,  $Sh$  enhances in the presence of heat absorbing source. Higher the dissipative heat larger  $\tau_x, \tau_z, Nu$  and  $Sh$  at the wall. It can be seen that increasing the Soret parameter  $S_0$  (or decreasing  $Du$ ) reduces  $\tau_x, \tau_z, Sh$  and enhances  $\tau_z, Nu$  at the wall  $\eta=0$ . An increase in slip parameter ( $A$ ) leads to reduction in  $\tau_x$  and enhancement in  $\tau_z, Nu$  and  $Sh$  while secondary slip ( $B$ ) exhibits an opposite behaviour on  $\tau_x, \tau_z, Nu$  and  $Sh$  on  $\eta=0$ .

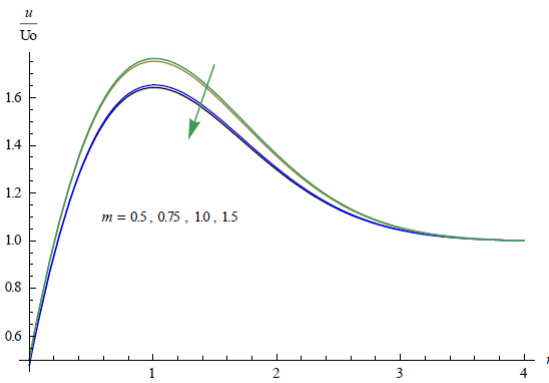


Fig.2a Variation of  $(u/U_o)$  with  $m$   
 $S_o=0.6, Du=0.1, N=0.5, Q=0.5, A=0.2, B=-0.02, Ec=0.01, R=0.5$

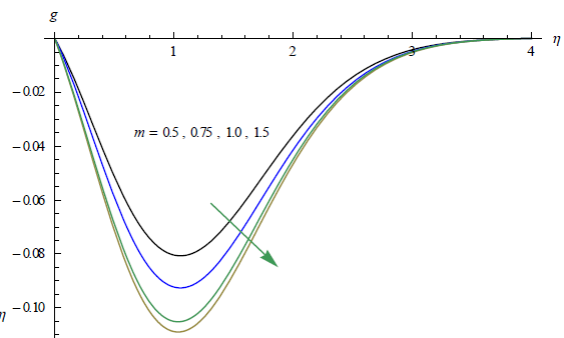


Fig.2b Variation of  $g$  with  $m$   
 $S_o=0.6, Du=0.1, N=0.5, Q=0.5, A=0.2, B=-0.02, Ec=0.01, R=0.5$

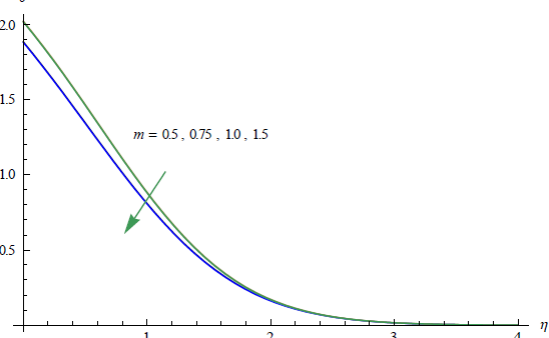


Fig.2c Variation of temperature( $\theta$ ) with  $m$   
 $S_o=0.6, Du=0.1, N=0.5, Q=0.5, A=0.2, B=-0.02, Ec=0.01, R=0.5$

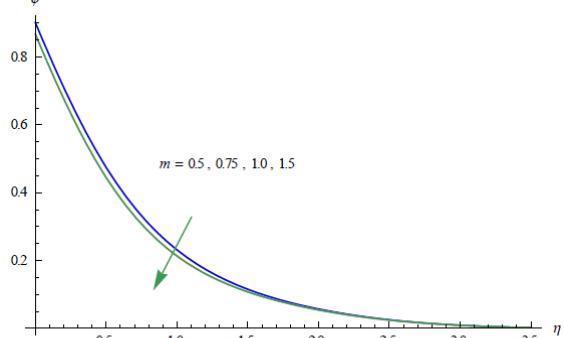


Fig.2d Variation of concentration( $\phi$ ) with  $m$   
 $S_o=0.6, Du=0.1, N=0.5, Q=0.5, A=0.2, B=-0.02, Ec=0.01, R=0.5$

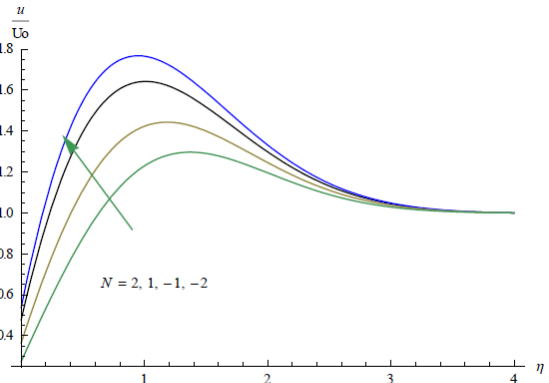


Fig.3a Variation of  $u/U_o$  with  $N$   
 $S_o=0.6, Du=0.1, N=0.5, Q=0.5, A=0.2, B=-0.02, Ec=0.01, R=0.5$

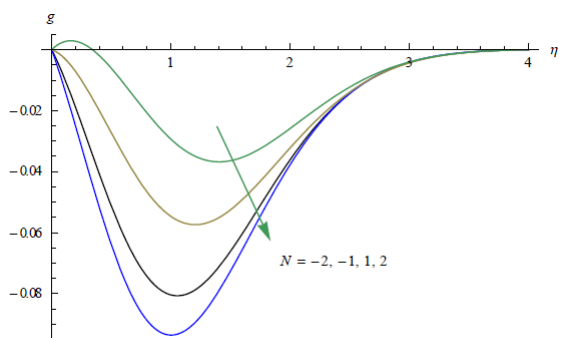


Fig.3b Variation of  $g$  with  $N$   
 $S_o=0.6, Du=0.1, m=0.5, Q=0.5, A=0.2, B=-0.02, Ec=0.01, R=0.5$

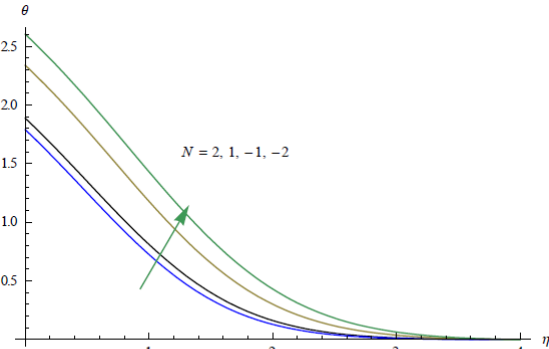


Fig.3c Variation of temperature( $\theta$ ) with  $N$   
 $S_o=0.6, Du=0.1, m=0.5, Q=0.5, A=0.2, B=-0.02, Ec=0.01, R=0.5$

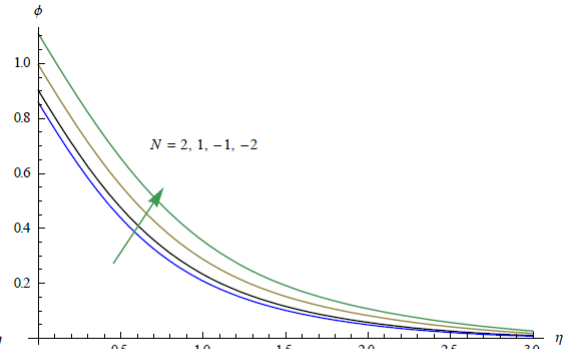


Fig.3d Variation of concentration( $\phi$ ) with  $N$   
 $S_o=0.6, Du=0.1, m=0.5, Q=0.5, A=0.2, B=-0.02, Ec=0.01, R=0.5$

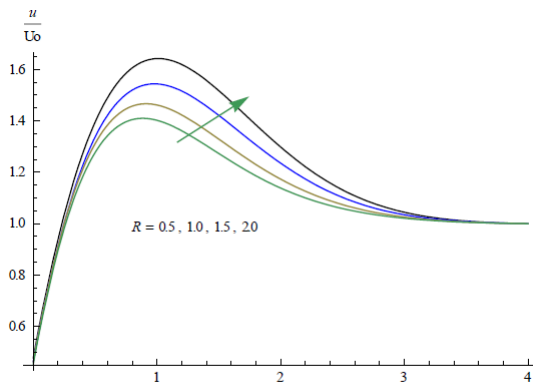


Fig.4a Variation of  $(u/U_0)$  with  $R$   
 $m=0.5, So=0.6, Du=0.1, N=0.5, Q=0.5, A=0.2, B=-0.02, Ec=0.01,$

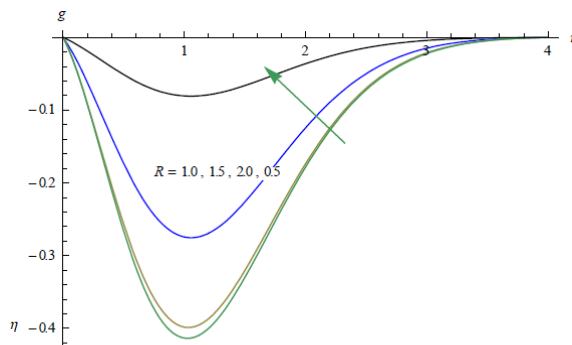


Fig.4b Variation of  $g$  with  $R$   
 $m=0.5, So=0.6, Du=0.1, N=0.5, Q=0.5, A=0.2, B=-0.02, Ec=0.01,$

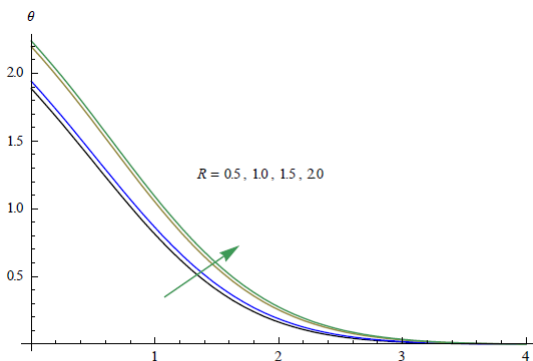


Fig.4c Variation of temperature( $\theta$ ) with  $R$   
 $m=0.5, So=0.6, Du=0.1, N=0.5, Q=0.5, A=0.2, B=-0.02, Ec=0.01,$

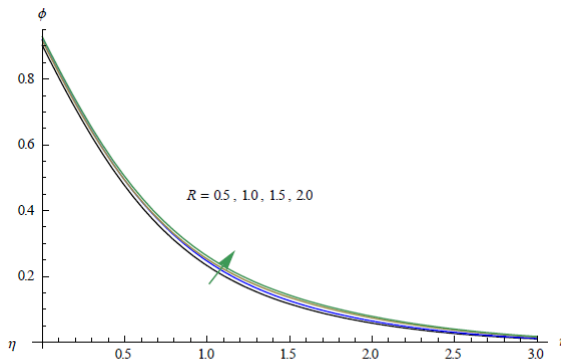


Fig.4d Variation of concentration( $\phi$ ) with  $R$   
 $m=0.5, So=0.6, Du=0.1, N=0.5, Q=0.5, A=0.2, B=-0.02, Ec=0.01,$

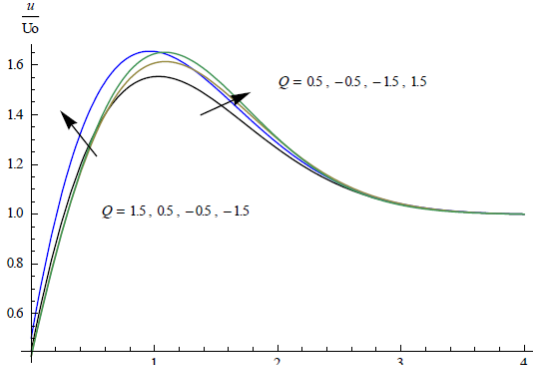


Fig.5a Variation of  $u/U_0$  with  $Q$   
 $m=0.5, So=0.6, Du=0.1, N=0.5, R=0.5, A=0.2, B=-0.02, Ec=0.01,$

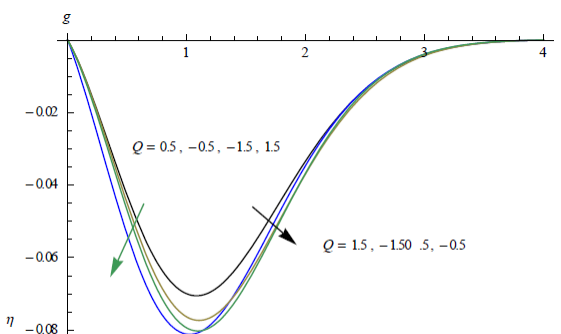


Fig.5b Variation of  $g$  with  $Q$   
 $m=0.5, So=0.6, Du=0.1, N=0.5, R=0.5, A=0.2, B=-0.02, Ec=0.01,$

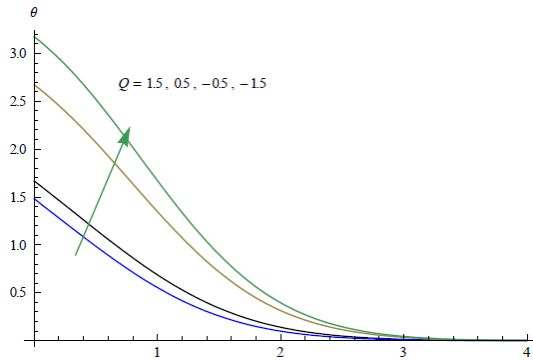


Fig.5c Variation of temperature( $\theta$ ) with  $Q$   
 $m=0.5, So=0.6, Du=0.1, N=0.5, R=0.5, A=0.2, B=-0.02, Ec=0.01,$

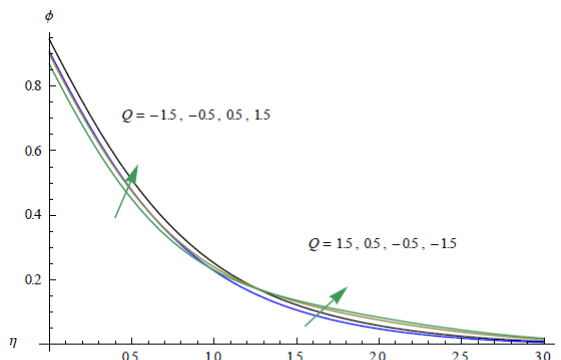


Fig.5d Variation of concentration( $\phi$ ) with  $Q$   
 $m=0.5, So=0.6, Du=0.1, N=0.5, R=0.5, A=0.2, B=-0.02, Ec=0.01,$



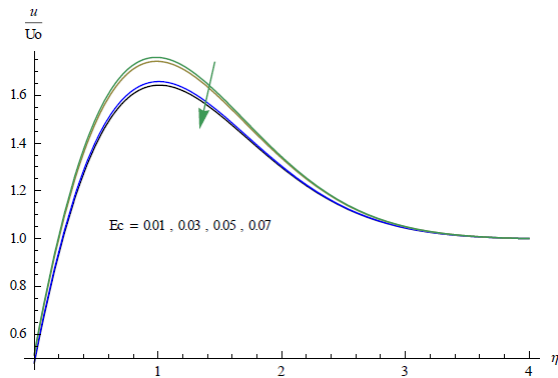


Fig. 6a Variation of  $u/U_o$  with  $Ec$   
 $m=0.5, So=0.6, Du=0.1, N=0.5, Q=0.5, A=0.2, B=-0.02, R=0.5,$

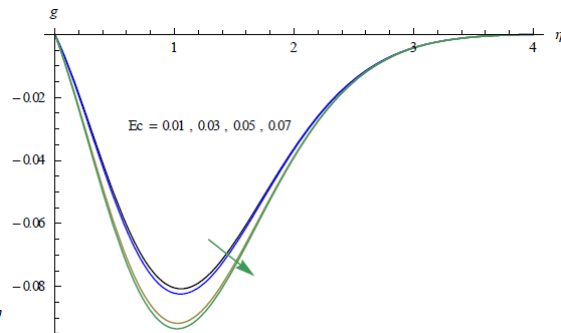


Fig. 6b Variation of  $g$  with  $Ec$   
 $m=0.5, So=0.6, Du=0.1, N=0.5, Q=0.5, A=0.2, B=-0.02, R=0.5$

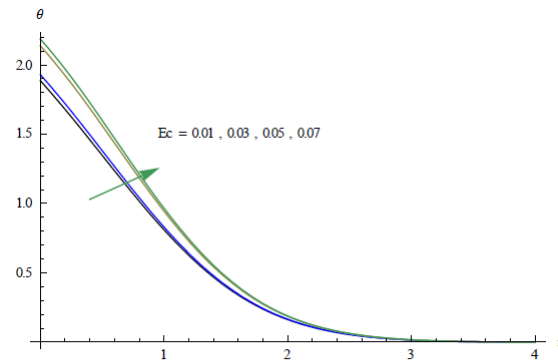


Fig. 6c Variation of temperature( $\theta$ ) with  $Ec$   
 $m=0.5, So=0.6, Du=0.1, N=0.5, Q=0.5, A=0.2, B=-0.02, R=0.5$

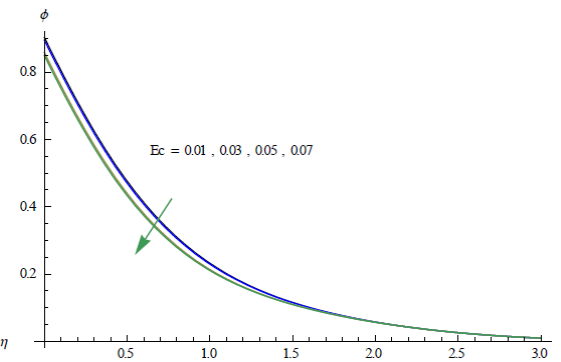


Fig. 6d Variation of concentration( $\phi$ ) with  $Ec$   
 $m=0.5, So=0.6, Du=0.1, N=0.5, Q=0.5, A=0.2, B=-0.02, R=0.5$

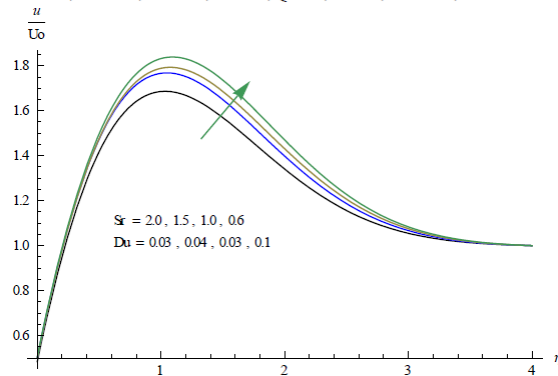


Fig. 7a Variation of  $u/U_o$  with  $Sr \& Du$   
 $m=0.5, R=0.5, N=0.5, Q=0.5, A=0.2, B=-0.02, Ec=0.01,$

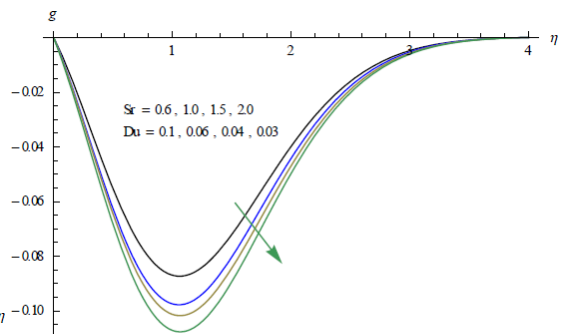


Fig. 7b Variation of  $g$  with  $Sr \& Du$   
 $m=0.5, R=0.5, N=0.5, Q=0.5, A=0.2, B=-0.02, Ec=0.01,$

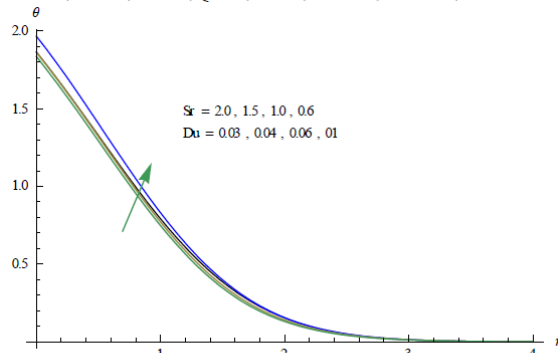


Fig. 7c Variation of temperature( $\theta$ ) with  $Sr \& Du$   
 $m=0.5, R=0.5, N=0.5, Q=0.5, A=0.2, B=-0.02, Ec=0.01,$

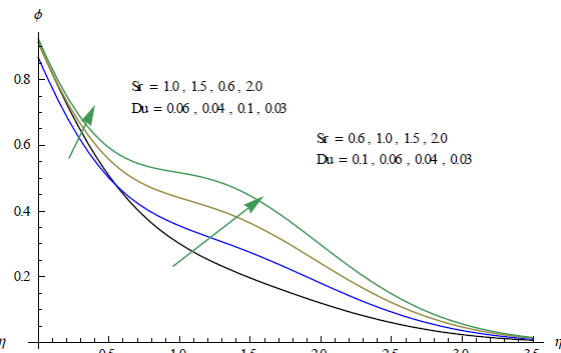


Fig. 7d Variation of concentration( $\phi$ ) with  $Sr \& Du$   
 $m=0.5, R=0.5, N=0.5, Q=0.5, A=0.2, B=-0.02, Ec=0.01,$

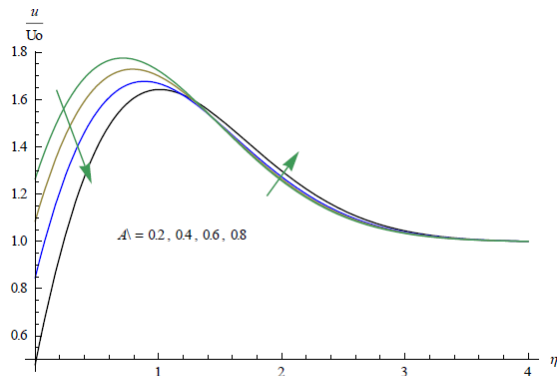


Fig.8a Variation of  $u/U_0$  with  $A$   
 $m=0.5, So=0.6, Du=0.1, N=0.5, Q=0.5, R=0.5, B=-0.02, Ec=0.01,$

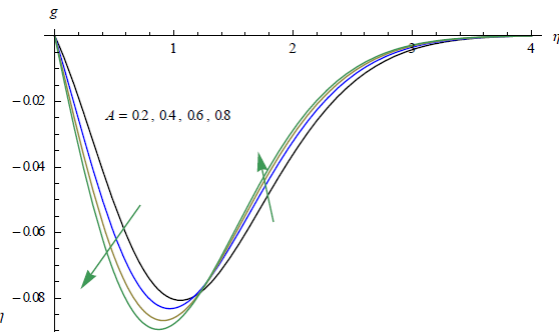


Fig.8b Variation of  $g$  with  $A$   
 $m=0.5, So=0.6, Du=0.1, N=0.5, Q=0.5, R=0.5, B=-0.02, Ec=0.01,$

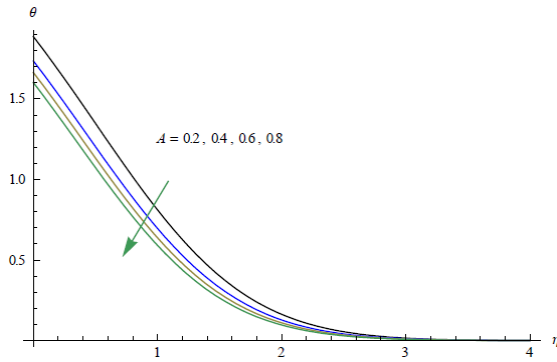


Fig.8c Variation of temperature( $\theta$ ) with  $A$   
 $m=0.5, So=0.6, Du=0.1, N=0.5, Q=0.5, R=0.5, B=-0.02, Ec=0.01,$

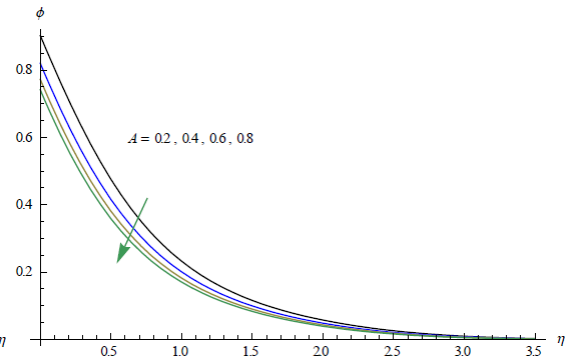


Fig.8d Variation of concentration( $\phi$ ) with  $A$   
 $m=0.5, So=0.6, Du=0.1, N=0.5, Q=0.5, R=0.5, B=-0.02, Ec=0.01,$

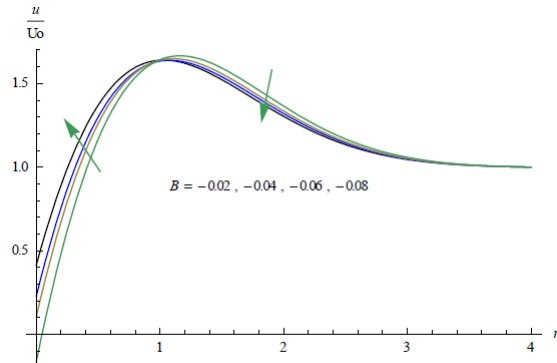


Fig.9a Variation of  $u/U_0$  with  $B$   
 $m=0.5, So=0.6, Du=0.1, N=0.5, Q=0.5, A=0.2, R=0.5, Ec=0.01,$

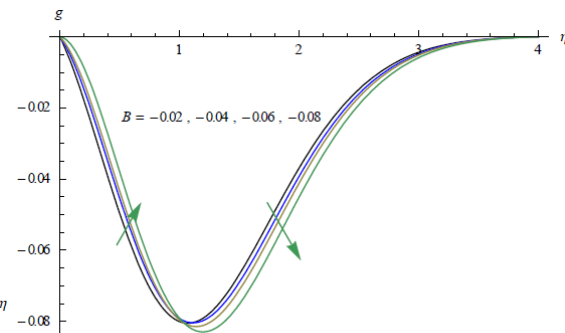


Fig.9b Variation of  $g$  with  $B$   
 $m=0.5, So=0.6, Du=0.1, N=0.5, Q=0.5, A=0.2, R=0.5, Ec=0.01,$

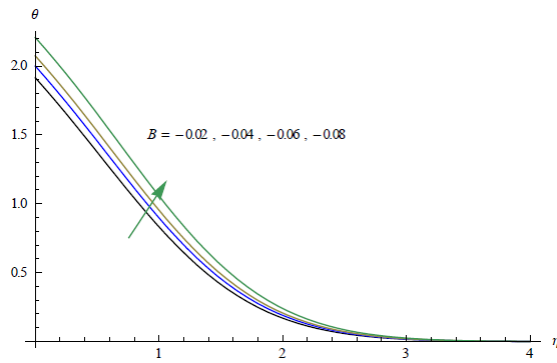


Fig.9c Variation of temperature( $\theta$ ) with  $B$   
 $m=0.5, So=0.6, Du=0.1, N=0.5, Q=0.5, A=0.2, R=0.5, Ec=0.01,$

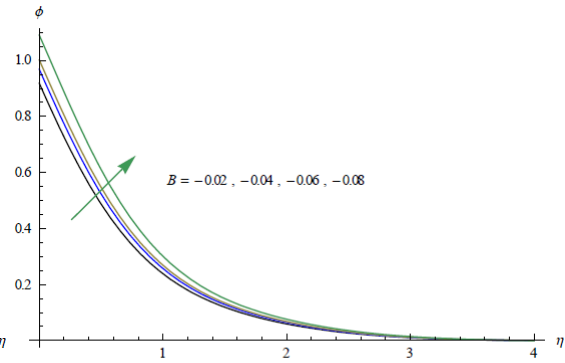


Fig.9d Variation of concentration( $\phi$ ) with  $B$   
 $m=0.5, So=0.6, Du=0.1, N=0.5, Q=0.5, A=0.2, R=0.5, Ec=0.01,$

Table – 2 : Skin Friction ( $\tau_x, \tau_z$ ), Nusslet number (Nu) and Sherwood Number (Sh) at  $\eta = 0$ 

Parameter	$\tau_x(0)$	$\tau_z(0)$	Nu(0)	Sh(0)	Parameter	$\tau_x(0)$	$\tau_z(0)$	Nu(0)	Sh(0)		
m	0.5	-2.5903	-0.0749297	0.530021	1.10822	Ec	0.01	-2.5903	-0.074929	0.530021	1.10822
	0.75	-2.6011	-0.0872738	0.531304	1.10979		0.03	-3.0099	-0.078328	0.518103	1.11824
	1	-2.7284	-0.0991142	0.5320387	1.11822		0.05	-4.6789	-0.083242	0.502629	1.13201
	1.5	-2.7321	-0.1092158	0.5327345	1.12142		0.07	-6.7897	-0.086747	0.491522	1.14254
N	0.5	-2.5903	-0.0749297	0.530021	1.10822	Q	0.5	-2.5903	-0.074929	0.530021	1.10822
	1.5	-2.9527	-0.107394	0.558883	1.16491		1.5	-2.6579	-0.13457	0.657989	1.15678
	-0.5	-1.8763	0.0049267	0.450837	0.962156		-0.5	-1.6759	-0.10679	0.467804	1.25678
	-1.5	-1.3308	0.0624066	0.395321	0.846855		-1.5	-1.4567	-0.08766	0.345467	1.35678
R	0.5	-2.5903	-0.0749297	0.530021	1.10822	A	0.2	-2.5903	-0.074929	0.530021	1.10822
	1	-2.6041	-0.145098	0.526487	1.10311		0.4	-2.0900	-0.11987	0.576185	1.2195
	1.5	-2.6205	-0.220904	0.514349	1.09537		0.6	-1.8688	-0.15161	0.60124	1.29491
	2	-2.6577	-0.263941	0.497829	1.07144		0.8	-1.6359	-0.17498	0.624539	1.34877
Sr/Du	0.6/0.1	-2.5903	-0.0829427	0.536094	1.09398	B	-0.02	-0.3456	-0.067304	0.522193	1.08872
	1.0/0.06	-2.0099	-0.0899627	0.541378	1.08161		-0.04	-0.4456	-0.045778	0.500149	1.0326
	1.5/0.05	-1.8977	-0.101556	0.546326	1.07484		-0.06	-0.8976	-0.033163	0.482288	0.998386
	2.0/0.03	-1.6790	-0.109367	0.554693	1.06094		-0.08	-1.0789	-0.237079	0.453185	0.917216

## 7. CONCLUSIONS

An attempt has been made to discuss the combined impact of rotation and Hall currents on convective heat and mass transfer flow of a viscous fluid through a porous medium past a stretching surface with second order slip. Using Finite element technique the governing equations have been solved. The important conclusion of this analysis are

- ❖ An increase in Hall parameter reduces the primary velocity, temperature, actual concentration and enhances the secondary velocity. The stress components, Nusselt and Sherwood number enhances with m.
- ❖ An increase in rotation parameter ( R ) enhances the primary velocity, temperature and concentration while the secondary velocity reduces with (m)in the flow region.  $\tau_x, \tau_z, Nu$  and Sh enhances with increasing values of R.
- ❖ The primary velocity, temperature, actual concentration reduces, secondary velocity increases with increase in N>0 and for N<0, a reversed effect is noticed.  $\tau_x, \tau_z, Nu$  and Sh enhances with N>0 and for N<0,  $\tau_x, Nu, Sh$  reduces,  $\tau_z$  enhances on  $\eta=0$ .
- ❖ Increase in So(or decrease in Du) reduces the primary velocity, temperature actual concentration while the secondary velocity enhances in the flow region. The stress component  $\tau_x, Sh$  reduce,  $\tau_y, Nu$  enhance with increase in So( or decrease in Du).
- ❖ Higher the dissipation smaller the velocities actual concentration and larger the temperature in the flow region.  $\tau_x, \tau_z, Nu, Sh$  enhance with Ec on the wall  $\eta=0$ .
- ❖ Higher the rotation parameter (R) larger the primary velocity, temperature, actual concentration and smaller the secondary velocity.  $\tau_x, \tau_z, Nu, Sh$  increase with R on the wall.
- ❖ An increase in first order Slip parameter (A) reduces the axial velocity ( $f'$ ), temperature, actual concentration and enhances the secondary velocity.  $\tau_x$  reduces and  $\tau_z, Nu, Sh$  enhances with A on  $\eta=0$ .
- ❖ An increase in second order slip(B)enhances the primary velocity, temperature, actual concentration, reduces the secondary velocity in the flow region.  $\tau_x, Sh$  enhances and  $\tau_z, Nu$  reduces  $\eta=0$  with increasing values of B.

## 8. REFERENCES

- [1]. Ahmed N and H.K. Sarmah : MHD Transient flow past an impulsively started infinite horizontal porous plate in a rotating system with hall current: Int J. of Appl. Math and Mech. 7(2) : 1-15, 2011.
- [2]. Alam, M.M and Sattar, M.A :Unsteady free convection and mass transfer flow in a rotating system with Hall currents, viscous dissipation and Joule heating ., Journal of Energy heat and mass transfer, V.22, pp.31-39(2000)
- [3]. Balasubramanyam M : Effect of radiation on convective Heat and Mass transfer flow in a horizontal rotating channel communicated to Research India Publications, India (2010).
- [4]. Bhattacharya K, Mukhopadyay S, Layek G :Similarity solution of mixed convective boundary layer slip flow over a vertical plate. Ain Shams Eng J, V.4, pp.299-305(2013)
- [5]. Circar and Mukharjee : Effects of mass transfer and rotation on flow past a porous plate in a porous medium with variable suction in slip flow. Acta Cienica Indica, V.34M, No.2, pp.737-751 (2008).
- [6]. Debnath, L: Exact solutions of unsteady hydrodynamic and hydromagnetic boundary layer equations in a rotating fluid system, ZAMM, V.55, p.431 (1975)
- [7]. Feidooniment N, Rashid MM, Mahmud S, Nazeeri F: Slip effects on MHD stagnation point flow and heat transfer over a porous rotating disk, Phys Sci. Int, V.5(1), pp.34-540(2015).
- [8]. Hayat T, Javed vT, Abbas Z: Slip flow and heat transfer of a second grade fluid past a stretching sheet through a porous medium, Int. J Heat Mass Transfer, V.51, pp.5428-4534(2008)

- [9]. Hazem Ali Attia : Unsteady MHD flow near a rotating porous disk with uniform suction or injection. Fluid dynamics Research, V.23, pp.283-290.
- [10]. Krishna,D.V,Prasada rao, D.R.V,Ramachandra Murty,A.S:Hydromagnetic convection flow through a porous medium in a rotating channel., J.Engg. Phy. and Thermo.Phy,V.75(2),pp.281-291(2).
- [11]. Mabood F, Das L:Melting heat transferton hydromagnetic flow of a nanofluid over a stretching sheet6 with radiation and second order slip.,Eur Phys J plus,1341,3(2016)
- [12]. Mabood F,Shaiq A,Hayat T,Abeloman S:Radiation effects on stagnation point flow with melting heat transfer ans second order slip.,Results in Physics,V.7,pp.31-42(2017)
- [13]. Madhavilatha,S and Prasada Rao D.R.V: Finite element analysis of convective heat and mass transfer flow past a vertical porous plate in a rotating fluid.,Int.Jour.Emerging and development,Vol.3,pp.202-216,(2017)
- [14]. Madhusudhan Reddy, Y, Prasada Rao, D.R.V : Effect of thermo diffusion and chemical reaction on non-darcy convective heat & mass transfer flow in a vertical channel with radiation. IJMA, V.4, pp.1-13 (2012).
- [15]. Malvandi A,Hedayat F,Gaqnji DD:Slip effects on unsteady stagnation point flow of a nanofluid over a stretching swheet.,Powder Technol,V.253,pp.377-384(2014)
- [16]. Mukhopadhyay S:MHD boundary layer slip flow along a stretching cylinder, Qin Shams. Eng J,V.4,pp.317-324(2013)
- [17]. Mukhopadhyay,S: Slip effects on MHD boundary layer flow over an exponentially stretching sheet with suction and thermal radiation, Ain Shams Eng J,V.4,pp.485-491 (2013)
- [18]. Pai, S.I : Magnetogas dynamics and Plasma dynamics. Springier Verlag, New York (1962).
- [19]. Rajasekhar, N.S, Prasad, P.M.V and Prasada Rao, D.R.V : Effect of Hall current , Thermal radiation and thermo diffusion on convective heat and mass transfer flow of a viscous, rotating fluid past a vertical porous plate embedded in a porous medium. Advances in Applied Science Research, V.3, No.6, pp.3438-3447 (2012).
- [20]. Rao,D.R.V and Krishna,D.V :Hall effects on unsteady hydromagnetic flow., Ind.J.Pure and Appl.Maths,V.12(2),pp.270-276(1981)
- [21]. Rashid MM,Kavyani MABeiman S:Investigation of entrophy generation in MHD and slip flow over a rotating porus disk with variable properties,Int.J.Heat Mass transfer,V.70,pp.892-917(2014)
- [22]. Sarojamma, G and Krishna, D.V : Transient Hydromagnetic convection flow in a rotating channel with porous boundaries. Acta Mechanica, V. 39, p.277 (1981).
- [23]. Sattar, M.A : Free and forced convection boundary layer flow through a porous medium with large suction. Int. J. of Energy Research, V.17, pp.1-17 (1993).
- [24]. Seth G.S. and Ghosh, S.K : Ind J. Eng. Sci., V.24, No.7, pp.1183-1193 (1986).
- [25]. Singh, K.D and Mathew : An oscillatory free convective MHD flow in a rotating vertical porous channel with heat sources. Ganita, V.60, No.1, pp.91-110 (2009).
- [26]. Sreerangavani, K, Rajeswara Rao,U and Prasada Rao, D.R.V : Effect of thermo-diffusion on MHD convection heat and mass transfer flow of chemically reacting fluid through a porous medium in a rotating system., Presented in 2nd International conference on Applications of Fluid dynamics, July, (2014)
- [27]. Sreevani,M : Mixed convective heat and mass transfer through a porous medium in channels with dissipative effects, Ph.D thesis, S.K.University, Anantapur , India (2002).
- [28]. Turkyilmazoglu M:Analytic heat and mass transfer of the mixed hydrodynamic/thermal slip MHD viscous flow over a stretched sheet.,Int.J.Mech Sci,V53,pp.886-896(2011)
- [29]. Turkyilmazoglu M:Multiple solutions of heat and mass transfer of MHD slip flow for the viscoelastic fluid over a stretching sheet.,Int.J.Therm SciV.50,pp.2264-2276,(2011).